AD_____

Award Number: W81XWH-12-1-0303

TITLE: Piezoelectric Composite Micromachined Multifrequency Transducers for High-Resolution, High-Contrast Ultrasound Imaging for Improved Prostate Cancer Assessment

PRINCIPAL INVESTIGATOR: Paul A. Dayton

CONTRACTING ORGANIZATION: University of North Carolina, Chapel Hill, NC 27599

REPORT DATE: August 2014

TYPE OF REPORT: Annual

PREPARED FOR: U.S. Army Medical Research and Materiel Command
                         Fort Detrick, Maryland 21702-5012

DISTRIBUTION STATEMENT: Approved for Public Release;
                         Distribution Unlimited

The views, opinions and/or findings contained in this report are those of the author(s) and should not be construed as an official Department of the Army position, policy or decision unless so designated by other documentation.

REPORT DOCUMENTATION PAGE

Form Approved
OMB No. 0704-0188

1. REPORT DATE	2. REPORT TYPE	3. DATES COVERED
August 2014	Annual	1 Aug 2013 – 31 Jul 2014

4. TITLE AND SUBTITLE
Piezoelectric Composite Micromachined Multifrequency Transducers for High-Resolution, High-Contrast Ultrasound Imaging for Improved Prostate Cancer Assessment

5a. CONTRACT NUMBER

5b. GRANT NUMBER
W81XWH-12-1-0303

5c. PROGRAM ELEMENT NUMBER

6. AUTHOR(S)
Paul A. Dayton and Xiaoning Jiang

E-Mail: padayton@email.unc.edu

5d. PROJECT NUMBER

5e. TASK NUMBER

5f. WORK UNIT NUMBER

7. PERFORMING ORGANIZATION NAME(S) AND ADDRESS(ES)
University of North Carolina, Chapel Hill
Chapel Hill, NC 27599-1350

8. PERFORMING ORGANIZATION REPORT NUMBER

9. SPONSORING / MONITORING AGENCY NAME(S) AND ADDRESS(ES)
U.S. Army Medical Research and Materiel Command
Fort Detrick, Maryland 21702-5012

10. SPONSOR/MONITOR'S ACRONYM(S)

11. SPONSOR/MONITOR'S REPORT NUMBER(S)

12. DISTRIBUTION / AVAILABILITY STATEMENT
Approved for Public Release; Distribution Unlimited

13. SUPPLEMENTARY NOTES

14. ABSTRACT

The objective of this proposal is to develop new technology for substantially improving the sensitivity of ultrasound to prostate cancer. This technology will be enabled by recent advances in ultrasound transducer fabrication techniques and ultrasound contrast imaging approaches. We hypothesize that a transrectal ultrasound probe utilizing a novel dual-frequency ultra-broadband approach will provide a new highly-sensitive diagnostic technique for prostate cancer imaging. Aim 1) Develop a new type of dual-frequency PC-MUT co-linear array with broad bandwidth to enable a new dual-frequency imaging technology for high-resolution, high sensitivity nonlinear transrectal contrast imaging. This probe will be fabricated using a new piezoelectric composite micromachined ultrasound transducer technology (PC-MUT), and by utilizing through-waver-via based multilayering technology. The final result will be a co-linear 2-D array configuration utilizing row-column electrodes. Aim 2) Assess the performance of new prototype array and imaging capability in (a) tissue mimicking and microvascular phantoms and in (b) a standard animal model of prostate cancer. In the preliminary in-vitro study, imaging resolution, contrast to tissue ratio, and lesion detectability will be assessed relative to a Siemens EV- 8C4 transrectal ultrasound probe. In the in-vivo study, molecular imaging and microvascular mapping will both be performed to assess the probe's ability Progress to date has included development of prototype single and multi-element array dual frequency transducers designed towards prostate imaging. Prototypes have been fabricated and tested and have demonstrated promising preliminary results.

15. SUBJECT TERMS-
Nothing Listed

16. SECURITY CLASSIFICATION OF:			17. LIMITATION OF ABSTRACT	18. NUMBER OF PAGES	19a. NAME OF RESPONSIBLE PERSON USAMRMC
a. REPORT	b. ABSTRACT	c. THIS PAGE			19b. TELEPHONE NUMBER *(include area code)*
U	U	U	UU	27	

Table of Contents

Introduction

Prostate cancer is challenging to assess with standard ultrasound. Our team has recently demonstrated a new approach of ultrasound imaging that uses a contrast agent with a dual-frequency transducer to produce high resolution images of microvascular structure. It is hypothesized that microvascular structure and density are related to degree of cancer, and that this new imaging approach may help us assess prostate cancer. However, to date, there are no dual-frequency transducers designed for prostate cancer imaging that can perform this high-resolution imaging approach. The objective of the proposed research is to design and test a dual-frequency transducer specifically for prostate cancer imaging using contrast agents.

Keywords

Ultrasound, acoustic angiography, dual-frequency, transducer, contrast agents, prostate

Acronyms

PC-MUT	Piezo Composite Micromachined Ultrasound Transducer
TRUS	Trans Rectal Ultrasound
KLM	Krimholtz–Leedom–Matthaei
PMN-PT	Lead Magnesium Niobate-Lead Titanate

Overall Project Summary

The original tasks as proposed are listed in blue, and the following black text details progress towards these tasks.

Aim 1) Develop a new type of dual-frequency PC-MUT co-linear array with broad bandwidth to enable a new dual-frequency imaging technology for high-resolution, high sensitivity nonlinear transrectal contrast imaging.

Task 1 PC-MUT co-linear array design (Months 1-12)
Extensive modeling will be performed to design 1D and 2D dual frequency (5 MHz/20 MHz) co-linear arrays. The pressure field with amplitude > 2 MPa at a few cm depth is expected from a 5 MHz array for effective microbubble excitation. A 20 MHz PC-MUT with -6dB bandwidth > 90% will be developed as the receiver and integrated with the 5 MHz transmitter for TRUS contrast imaging.

Methods and Results for Task 1: Progress towards Task 1 was reported in the prior progress report. Some updated highlights are provided below:

Design of single-element 1D PC-MUT transducers:

A single element dual frequency transducer was developed first to verify the detection of super harmonic responses from microbubbles excited by low frequency ultrasound. The low frequency transmitter for contrast-enhanced super harmonic imaging is required to exhibit not only high negative pressure but also short ringing near the resonant frequency of microbubbles. However, due to the spatial and frequency limitation in many interventional ultrasound imaging probes, a conventional transmitter design with a thick and lossy backing layer for a short ringing at a low frequency is not practical. Therefore, a new design concept considering optimal matching, backing, and isolation layers as well as the active layers is required for the dual-frequency ultrasound enabled super harmonic imaging.

The schematic design of the single element dual-frequency transducer is shown in . In this research, the low frequency transmitter without backing material was designed to reduce the total thickness. To redeem a narrow bandwidth due to the absence of the backing layer, 1-3 piezoelectric composite was used as an active material of the transmitter. In the aspect of the receiver, wideband performance is also required for the efficient detection of the high-frequency and broadband harmonics scattered from micro-bubbles. Thus, the 1-3 piezo composite was used for a receiver with broad bandwidth. If both transmitter and receiver are made of piezoelectric composites with relatively low acoustic impedance (~19 MRayl), the isolation layer between the low frequency transmitter and the high frequency receiver should be carefully designed for efficient acoustic wave propagation. Due to the low acoustic impedance of the composites, conventional epoxy materials based isolation layer design cannot make a large enough

impedance difference at the boundary between two composites [1]. Therefore, a dual-layer design was adopted for the isolation layer.
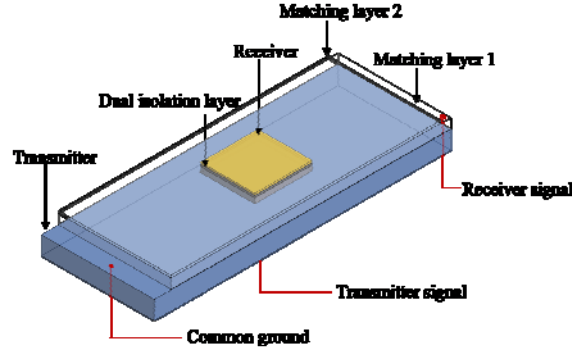

Figure 1. Schematic view of a dual frequency TRUS transducer design.

Single element design with KLM modeling

The dimensions of each part were designed by using a Krimholtz–Leedom–Matthaei (KLM) model. Although our original proposal involved a 5 MHz transmitter, we have revised our design to utilize a 2 MHz transmitter based on more recent data showing improved signal to noise at this lower frequency. The material properties and dimensions of designed components are listed in . A steel shim was used as a second isolation layer which is next the transmitter due to its high acoustic impedance (~50 MRayl). The large difference between acoustic impedance of isolation layers 1 and 2 can provide a strong reflection of received high frequency waves at the boundary. Although this reflection may slightly reduce the receiving bandwidth, the isolation layers would block the wave transmission to the transmitter and backscattered wave from the backside of the transmitter. The thickness of both isolation layers was selected as a quarter wavelength, and then adjusted by analyzing pulse echo amplitude and bandwidth using the KLM model. The simulation results are shown in . A slight degradation of the transmitting performance can be estimated due to isolation layer in front of the radiation area, but its area is just small portion of the low frequency radiation area (~14 %). Moreover, the thickness of the isolation layer is negligible (less than 1/20 wavelength) of the for the designed low frequency transmission.

Table 1. Parameters of single element dual frequency transducer.

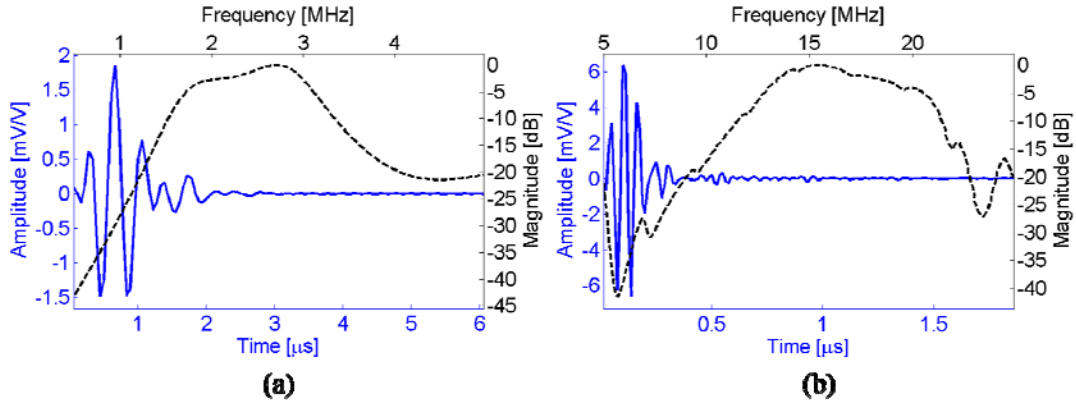|	Material	Density (kg/m^3)	Acoustic impedance (MRayl)	Dimension (mm^3)
Transmitter	1-3 composite	5300	19.1	3.8×8.0×0.71
Receiver	1-3 composite	5450	20.0	2.0×2.0×0.08
Matching layer	Al_2O_3/epoxy	2900	5.80	3.8×8.0×0.30
Isolation layer 1	E-solder 3022	2600	5.50	2.0×2.0×0.05
Isolation layer 2	Steel	8840	51.7	2.0×2.0×0.08

Figure 2. Impulse responses from KLM model for the single element dual frequency TRUS transducer: (a) impulse results for the transmitter (b) impulse results for the receiver.

The peak-to-peak voltage and -6dB bandwidth were for both transmitter and receiver were calculated from the pulse-echo modeling results. The transmit excitation response was calculated using KLM model to estimate the achievable peak negative pressure value. The calculated peak negative pressure was 6.1 kPa with the 2 cycles of 1 V_{pp} sinusoidal excitation, thus about 1.8 MPa negative pressure can be generated with 2 cycles of 300 V_{pp} sinusoidal excitation. The designed transmitter showed the loop sensitivity of 3.4 mV_{pp}/V and the -6dB fractional bandwidth of 61.2 %. The high-frequency receiver exhibited the sensitivity and bandwidth of 12 mV_{pp}/V and 49.3 %, respectively. Based on previous experimental results, it is reasonable to develop a dual frequency linear array with the same configuration utilizing a 2 MHz transmitter and 20 MHz receiver.
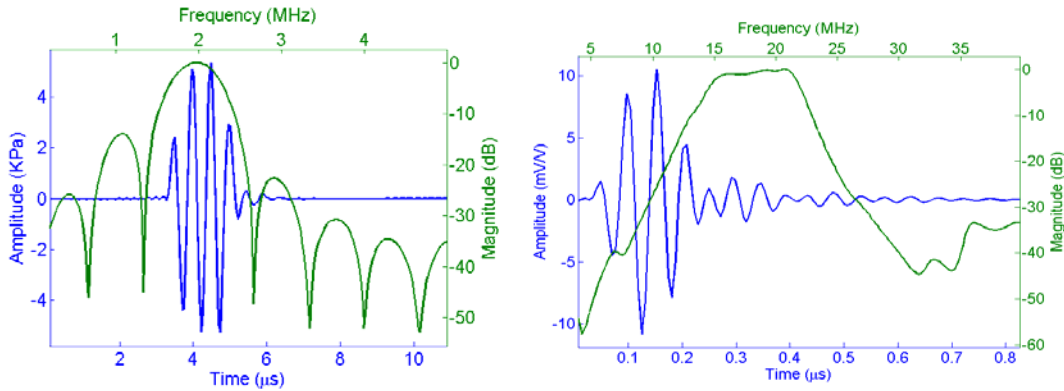
Multi element array design and modeling

Figure 3. Transmit excitation response of low frequency (5MHz) element in longitudinal mode (left) and Pulse-echo response of high frequency (20MHz) element in longitudinal mode (right).

The KLM model was used to estimate the performance of elements in the linear array. The transmit excitation performance at 2 MHz and pulse-echo response at 20 MHz were modeled considering different matching and backing materials. Low frequency transmitting (2 MHz) and high frequency receiving (20 MHz) configurations were simulated separately (Figure 3)). An isolation layer of Ni and Alumina/epoxy were used to improve the performance. The detailed

parameters and corresponding simulation results were summarized in . The pressure field was then investigated for the array. Field II, a Matlab toolkit (Matlab, The Mathworks Inc., Natick, MA), was used for the field simulation to determine the pitch size and group firing scheme. Figure 4 shows the pressure information in 2 MHz transmitting (left) and 20 MHz receiving (right). The focus was set at 40 mm far from the probe. With phased delay set-up, the -6 dB beam width at low frequency reaches 1.4 mm, and 0.5 mm at high frequency receiving. The array design specifications were summarized in Table 3.

Table 2 Design parameters of each element in the array

	2 MHz	**20 MHz**
Aperture	12 mm by 730 μm	6 mm by 180 μm
Backing Layer	-	Alumina (25μm) / Ni (80 μm)
Active Material	1-3 composite (770 μm)	PMN-PT (100 μm)
Matching Layer	Alumina (200 μm)	Alumina (30 μm)

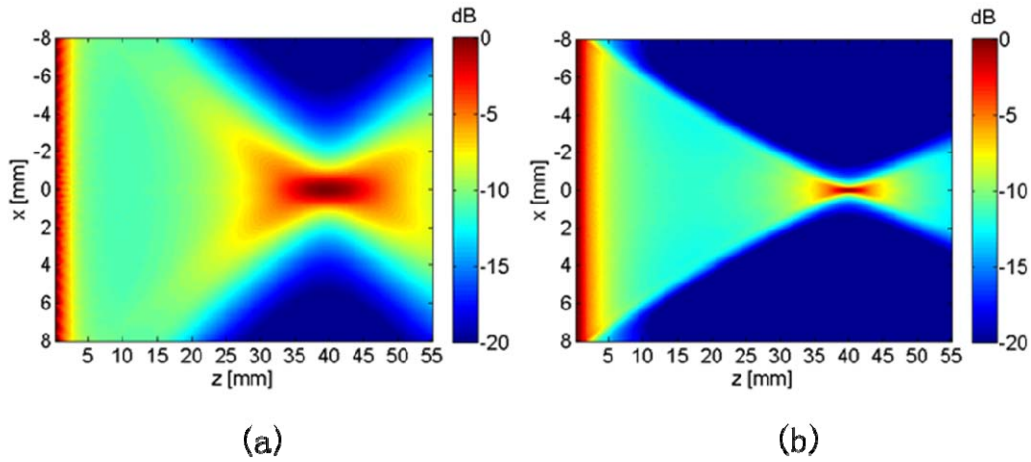(a)   (b)

Figure 4. Beam profile in 2 MHz transmitting (a) and 20 MHz receiving (b), focus at 40 mm.

Table 3 Array Design parameters of each layer configuration

Aperture	17.5 mm by 12 mm	
Working mode	Transmitting (2 MHz)	Receiving (20 MHz)
Pitch	730 μm (0.75 λ)	180 μm (1 λ)
Element number	24	96
Material	1-3 Composite	PMN-PT single crystal

Dual frequency co-linear array fabrication processes will be developed under this task for dual frequency co-linear array prototyping. At the end of this task, a co-linear array with 64-element 5 MHz 1D array and 128-element 20 MHz 1D array will be fabricated for demonstration of dual frequency PC-MUT co-linear array technology.

Subtask 2.1 1-3 piezocomposite fabrication (Months 3-6)
The fabrication of 20 MHz PC-MUT receivers will follow the standard PC-MUT fabrication process. For the 5 MHz PC-MUT transmitter, PIN-PMN-PT 1-3 composite will be fabricated using dice-and-fill process. The electromechanical coupling coefficient of fabricated 1-3 piezo composites are expected to be > 0.75.

Subtask 2.2 Multilayering process (Months 6-12)
Conductive through-wafer-vias (TWV) process will be developed for multilayer transducer demonstration. Bonding process for single layer and multilayer dual frequency co-linear array fabrication will be developed under this subtask.

Subtask 2.3 Dual frequency co-linear array prototyping (Months 12-21)
The 5 MHz composite layer will be fabricated first, followed by attachment of the 20 MHz receiver and matching layers. The bonded co-linear array acoustic stack will then be wired and tested.

Methods and Results for Task 2:

Prototype dual-frequency piezoelectric composite (PC-MUT) single element fabrication

Based on the design parameters, the prototypes of dual frequency transducer were fabricated. At first, the dual isolation layers were fabricated using E-solder and a steel shim. The E-solder (Von Roll Isola, Inc., New Haven, CT) was pasted on the one side of the steel shim which has a designed thickness of 80 μm and cured for 10 hours at 45°C, and then, shaped to 2.0×2.0 mm^2 which is similar to the size of the receiver aperture. The E-solder side was lapped down to the designed thickness of 50 μm. The steel side was attached to the low frequency transmitter and E-solder side was attached to the high frequency receiver using Epo-tek 301 (Epoxy Technology Inc., Billerica, MA). For the transmitter, PMN-PT/epoxy 1-3 composites with the volume fraction of 65 % and a pitch of 430 μm was used. Another 1-3 composite (volume fraction of 75 % and a pitch of 60 μm) was used as a receiver material. The matching layer material (Epo-tek 301 mixed with 0.3 micron Al_2O_3 powders) was poured on the front side of the transmitter submerging the receiving part. The cured matching layer part was then lapped until the high frequency composite part was exposed. The gold electrode was next deposited on the lapped surface to form a common ground. The matching layer of the receiver was fabricated using the similar process of transmitter's matching layer fabrication. The back side of the low frequency composite was attached to the tip of a syringe which is used as a support fixture. As a final step, the wires were connected and both high and low frequency composites were re-poled. Figure 5 shows the fabricated prototypes. The difference between prototype 1 and 2 is the aperture size of

the receiver. The receiving aperture of prototype 1 was modified to 3.8×2.0 mm^2 from the designed dimension in Table 1 to validate the appropriate size of the receiver in a stacked dual-frequency transducer structure, whereas the receiving aperture of prototype 2 was 2.0×2.0 mm^2.
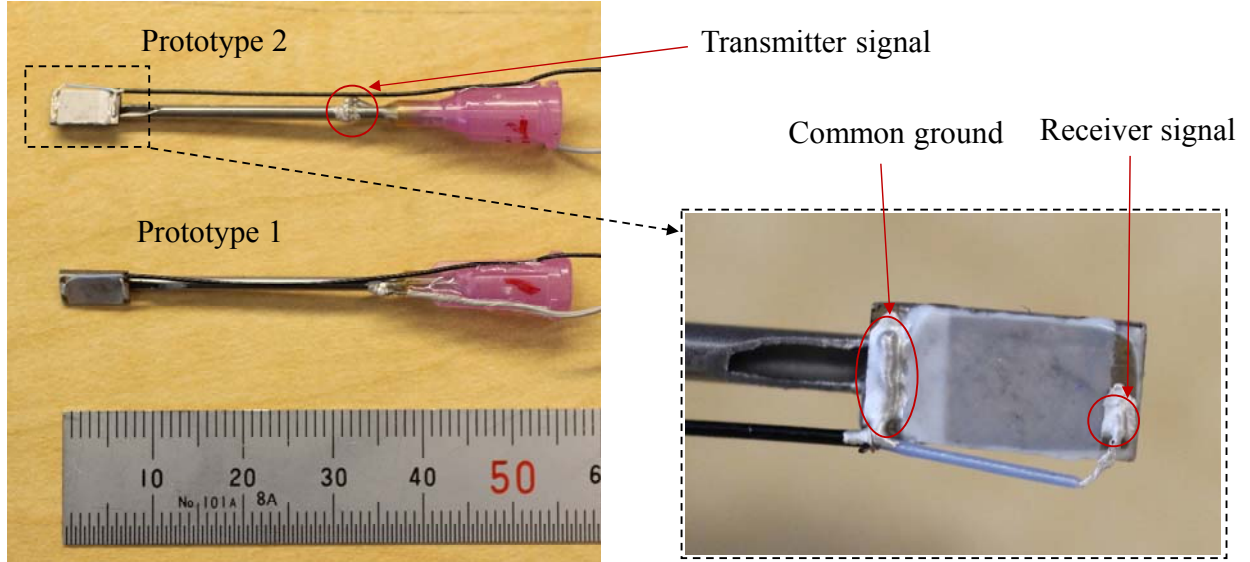

Figure 5. Photograph pictures of dual-frequency transducer prototypes.

Prototype dual-frequency PC-MUT array fabrication

There are several options for dual layer linear array fabrication, and the method adopted in this research was the bonding-and-dicing technique. The bonding process was performed first (Figure 6). The 1-3 composite was used as 2 MHz transmission active material. The thickness is around 770 μm, and aperture size is 12 mm by 17.5 mm. The dual isolation layers, nickel and alumina/epoxy, were laminated one by one (Figure 7). First, the Nickel layer was electro-plated with the thickness of ~80 μm. Alumina powders and epoxy were mixed using a centrifuge pump (Microfuge Lite, Beckmancoulter, CA, US), and the mixtures were casted onto the electroplated Ni and cured at 60 ℃ for 10 hours. The Alumina/epoxy layer was then lapped down to ~30 μm. After that, a layer of active material PMN-PT single crystal with the dimension of 6 mm x 17.5 mm x 110 μm was bonded to the isolation layer using Epo-Tek 301epoxy (Epoxy Technology Inc., Billerica, MA, USA). The Last, the matching layer of Alumina/epoxy with ~25 μm thickness was casted to cover the whole aperture.
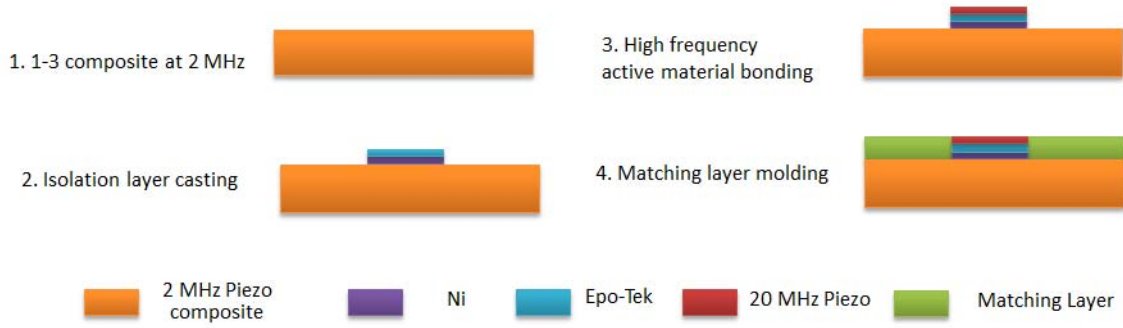
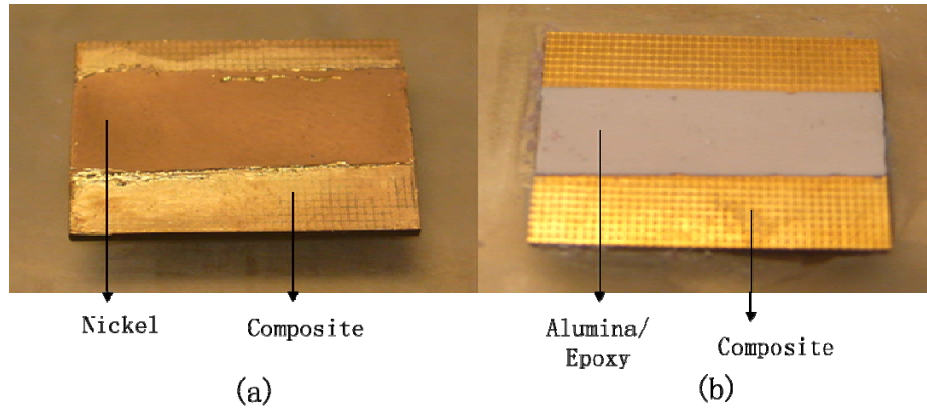**Figure 6.** Bonding process for linear array fabrication.

Figure 7. Photograph pictures of linear array prototypes with isolation layers attached. (a) electro-plated nickel; (b) alumina/epoxy bonded and lapped.

Since the pitch size is different for transmission and receiving arrays, the dicing was conducted individually for each array (Figure 8). For the high frequency receiving array, the dicing depth was ~130 μm. The pitch size and kerf are 180 μm and 30 μm, respectively. For the low frequency transmitter, the dicing depth was ~800 μm, the pitch size and kerf are 730 μm and 30 μm, respectively.
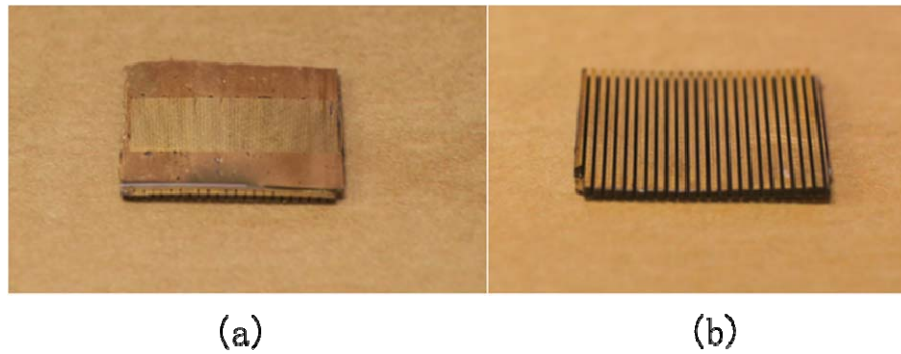
Figure 8. Photograph pictures of a diced array. (a) Top view - high frequency; (b) bottom view – low frequency

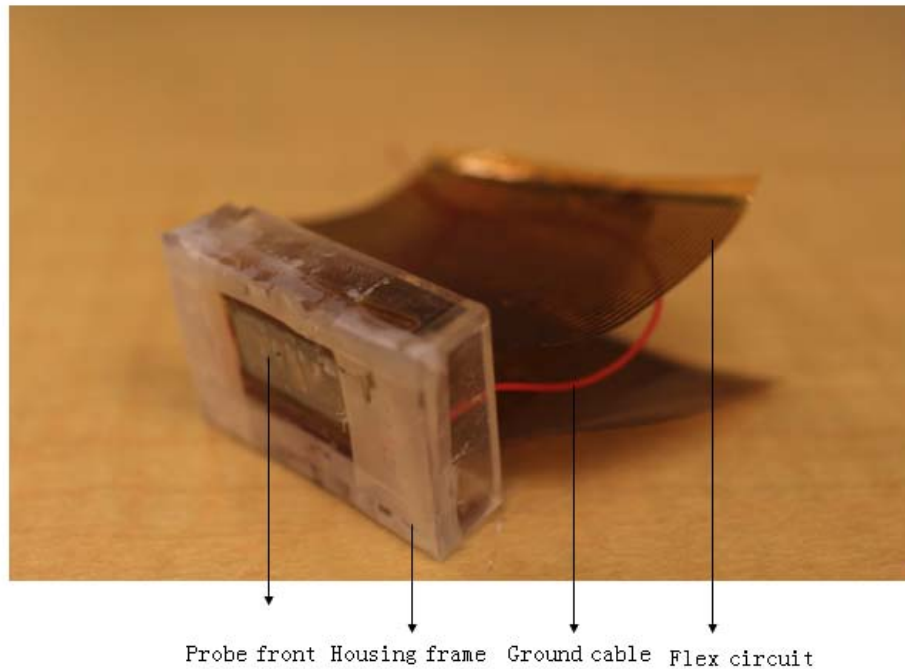After the array was diced, the flex-circuit was bonded onto the array and the housing was attached. (Figure 9)

Probe front   Housing frame   Ground cable   Flex circuit

Figure 9. The prototyped dual frequency linear array.

Task 3 Characterization of dual frequency PC-MUT co-linear array (Months 15-27)
Electrical and acoustic characterizations will be performed under this task to evaluate the prototyped dual frequency co-linear array.

Subtask 3.1 Electrical characterization (Months 15-21)
Resonant frequency, capacitance, and electrical impedance of single element and a group of elements will be measured using an impedance analyzer. The measured values will be compared with the modeling results.

Subtask 3.2 Acoustic characterization (Months 21-27)
Transducer characterization will be performed under this subtask. The prototype array will be driven with the multi-channel Verasonics programmable ultrasound pulser/receiver). Pulse-echo and hydrophone (HNC-0200, Onda Corp) characterization will be performed in water tank to obtain the transmission characteristics of the 5 MHz transmitter, and the receiving sensitivity and bandwidth of the 20 MHz receiver.

Methods and Results for Task 3:

Electrical Characterization of single element prototype

The electrical impedance of both transmitters and receivers of the prototypes were measured using an Agilent 4294A precision impedance analyzer (Agilent Technologies Inc., Santa Clara, CA). Figure 10 and Figure 11 show the electrical impedance and phase spectra of prototype 1 and prototype 2, respectively. Both prototypes showed the transmitting and receiving frequencies at the designed ranges.
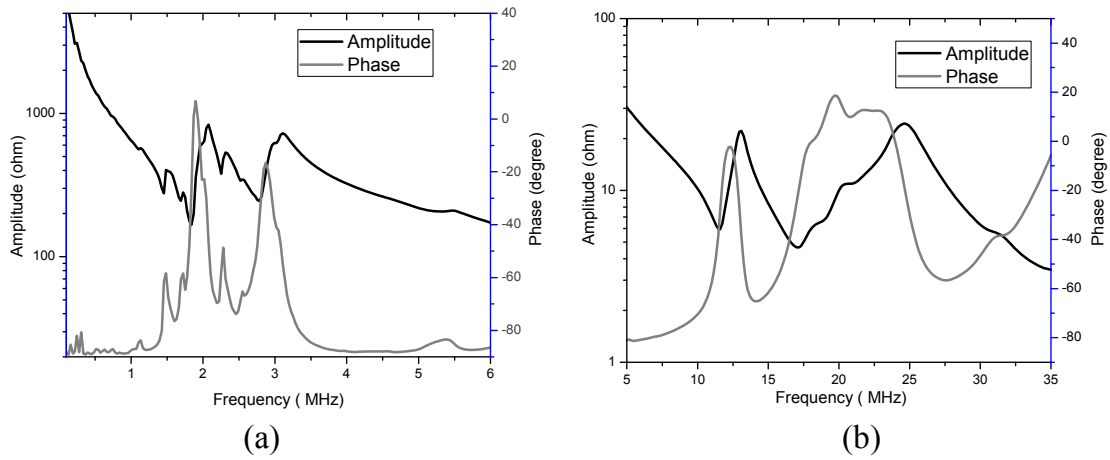

Figure 10. Impedance and phase spectra of the prototype 1: (a) Transmitter; (b) Receiver.
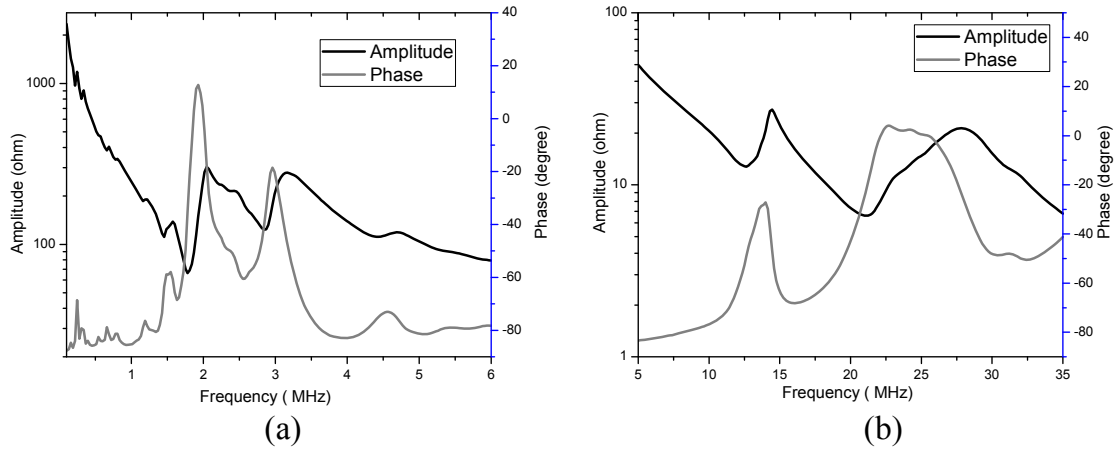

Figure 11. Impedance and phase spectra of the prototype 2: (a) Transmitter; (b) Receiver.

Electrical characterization of array prototype

The electrical impedance of selected elements of the array were measured using an Agilent 4294A precision impedance analyzer (Agilent Technologies Inc., Santa Clara, CA). The transmission element exhibits the fundamental resonant frequency of 2.2 MHz, and the resonant and anti-resonant frequencies of the receiving part are 20 MHz and 24 MHz, respectively (Figure 12).
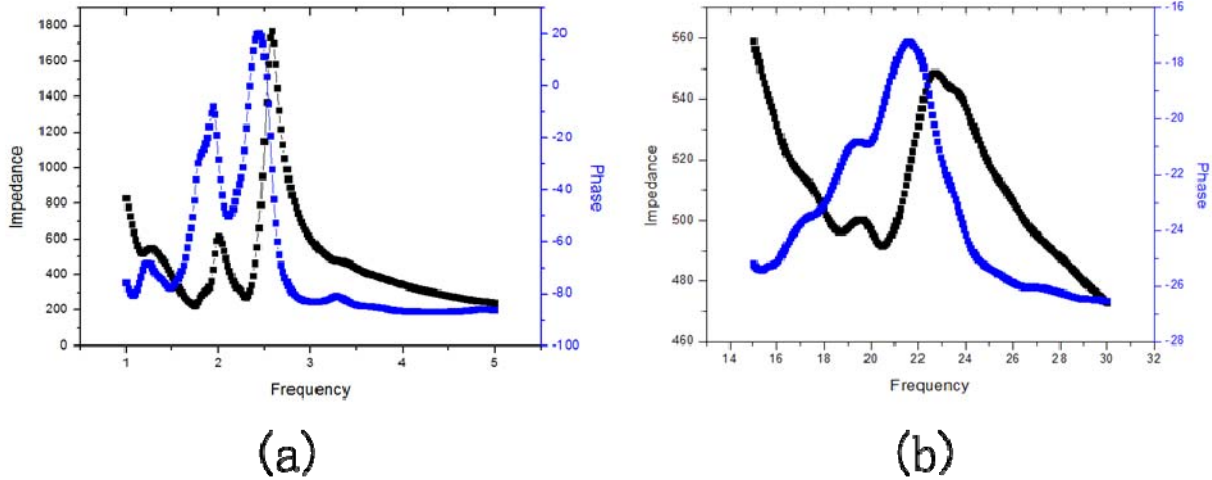

Figure 12. Electrical response of transducer at transmission (a) and receiving (b)

Acoustic characterization of single element prototype

The transmitting and receiving performances of prototypes were tested. The pulse-echo signals of both transmitters and the receivers were measured individually and the peak negative pressure value of the transmitters were also measured. A pulser/receiver (5900PR, Panametrics Inc., Waltham, MA) was used in pulse-echo test and energy of 1 µJ and 2 µJ were excited to the receiver and transmitter, respectively. The cut-off frequency of the low-pass filter was 20 MHz for the transmitter and 50 MHz for the receiver test. The gain and attenuation were not changed during the pulse-echo test. The transmitter of the prototype 1 showed the peak-to-peak voltage of 210 mV and -6 dB bandwidth of 61.1 %, and the receiver showed the peak received echo voltage 430 mV and -6 dB fractional bandwidth of 45.1 % (Figure 13). The pulse-echo results of the prototype 2 is shown in Figure 14. The measured echo peak voltages for the transmitter and receiver are 430 mV$_{pp}$ and 410 mV$_{pp}$, respectively. The measured -6dB fractional bandwidth for transmitter and receiver were 55.1% and 35.6 %, respectively.
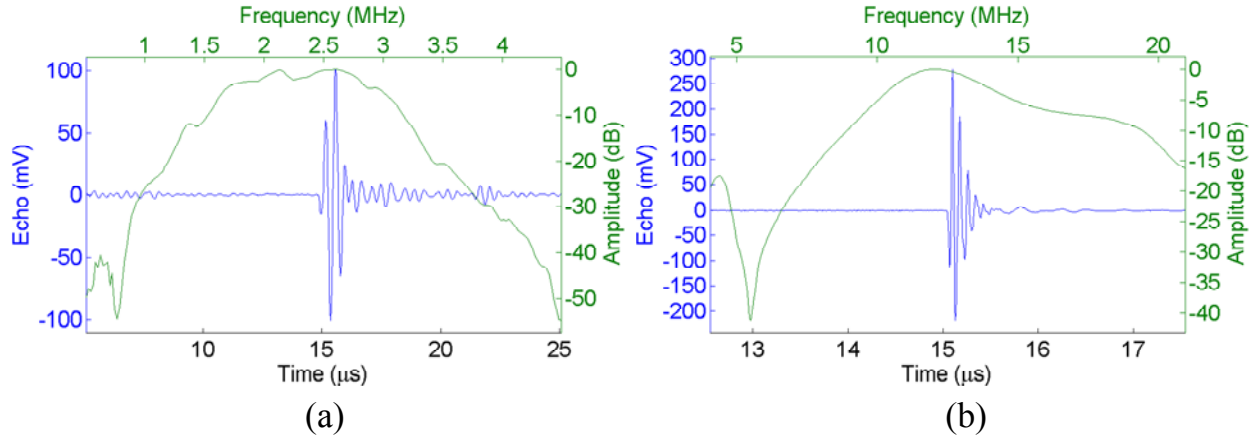
Figure 13. Pulse-echo responses and spectra of the prototype 1: (a) Transmitter, (b) Receiver.
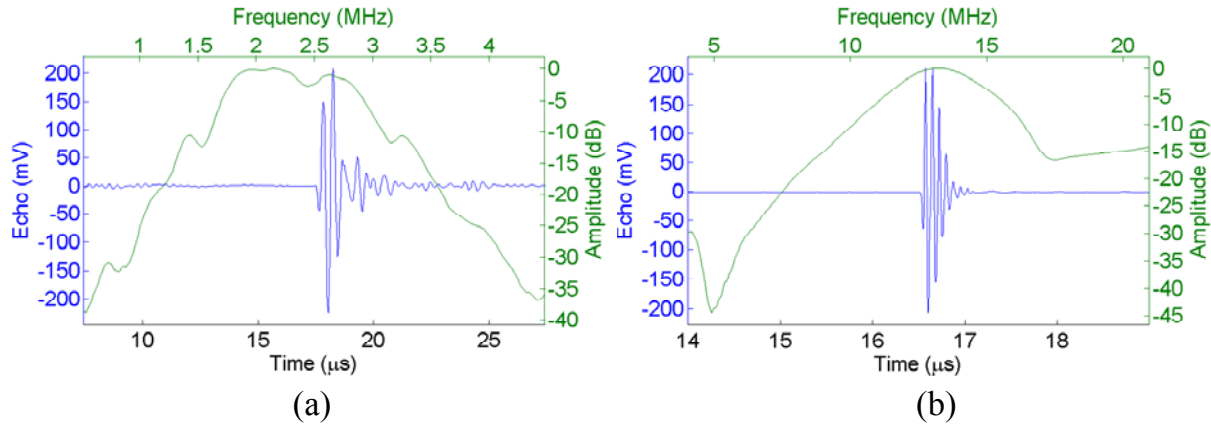

Figure 14. Pulse-echo resposnes and spectra of the prototype 2: (a) Transmitter, (b) Receiver.

The peak negative pressure of prototype 2 was measured using the setup shown in Figure 15. In the set-up, a needle hydrophone (HNA-0400, Onda Corp., Sunnyvale, CA) was located in front the prototyped transducer. The transmitter of the prototype 2 was excited with two cycles of 2 MHz and 300 mV$_{pp}$ sinusoidal input by a function generator (AFG3101, Tektronix Inc., Beaverton, OR) and amplified by 55 dB using a radio-frequency amplifier (Model 3200L, Electronic Navigation Industries Inc., Rochester, NY). The hydrophone was moved laterally and axially and the measured pressure values were processed to obtain the pressure mapping, as shown in Figure 16. The peak negative pressure at the far field was about -1.6 MPa, which is high enough to excite microbubbles for nonlinear responses. The mechanical index (MI) was calculated to be 1.13, which is within regulated FDA limits for diagnostic ultrasound equipment.
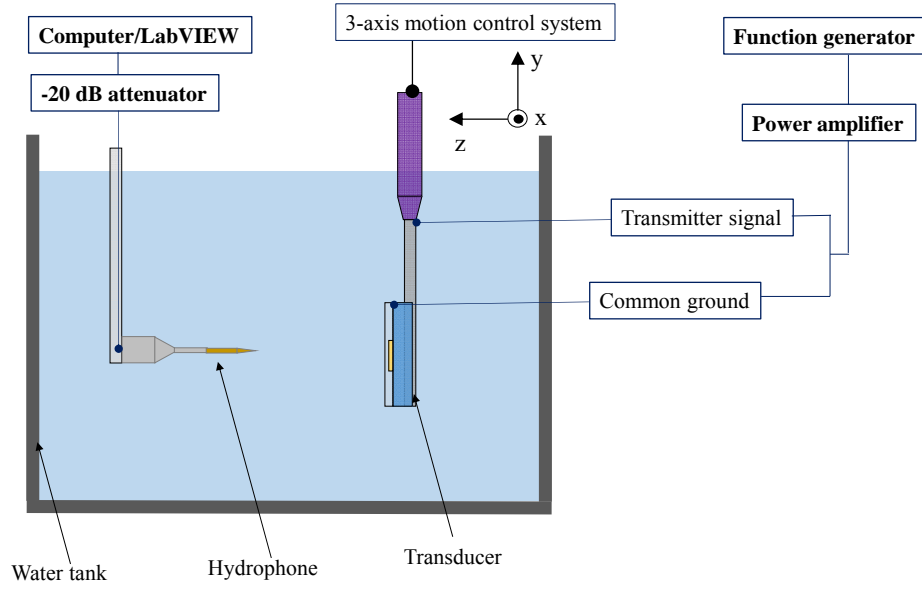
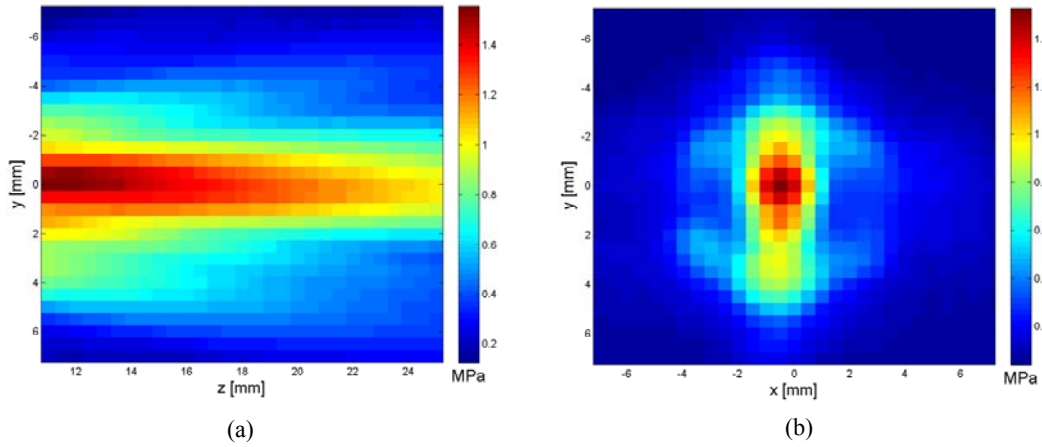**Figure 15.** Pressure mapping measurement setup.

(a)

(b)

Figure 16. Pressure mapping results for the prototype 2 transducer (with 2 cycles of the 2 MHz and 300V$_{pp}$ excition): (a) yz-plane; (b) xy-plane at z = 13 mm.

Acoustic characterization of array prototype

The transmitting and receiving performances of array elements were tested using the pulser/receiver (5900PR and 5077PR, Panametrics Inc., Waltham, MA). The low frequency transmission elements were excited by a 200 V pulse, and showed a peak-to-peak voltage of 70 mV and -6 dB bandwidth of ~45%. The receiving element was excited by 1 μJ pulse and showed ~ 300 mV$_{pp}$ response and ~50% in -6 dB bandwidth , respectively (Figure 17).
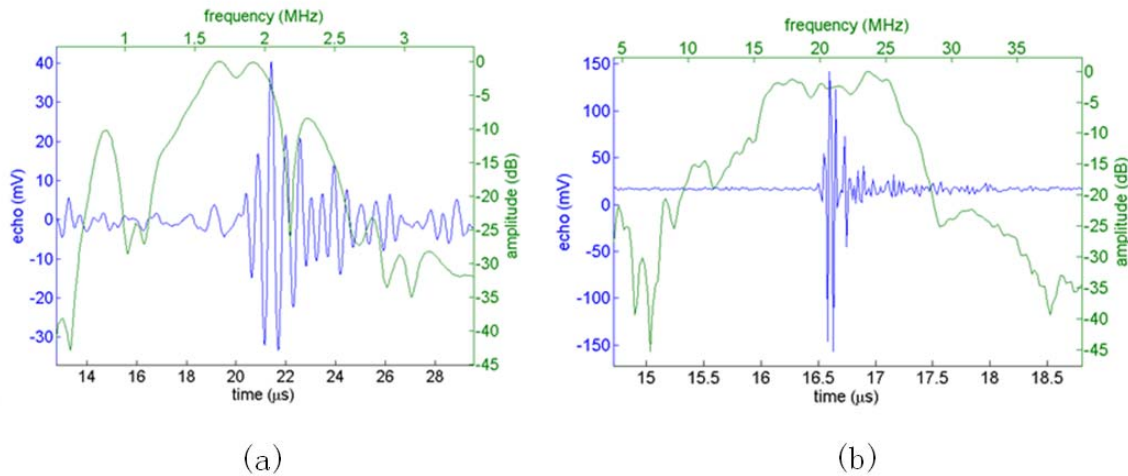
Figure 17. Pulse-echo response of transducers at transmission (a) and receiving (b)

Task 4 Prepare manuscript for data dissemination (Months 30-33)
After completion and characterization of the prototype array transducer, data will be presented in a manuscript for a peer-reviewed journal such as IEEE Ultrasonics, Ferroelectrics, and Frequency Control.

Task 4 is to be completed in year 3. No progress yet to report

Task 5 In-vitro testing of dual frequency PC-MUT co-linear array (Months 21-30)
Subtask 5.1 Tissue phantom testing (Months 21-25)
Gelatin based tissue mimicking phantoms will be used with a range of spherical hyperechoic and hypoechoic lesions. A spectrum of lesion detectability parameters will be tested. These lesions will be imaged at several axial depths using our prototype array and the Siemens EV-8C4 clinical TRUS probe. A blinded reader study will be performed and accuracy of the manually defined regions will be assessed between clinical and prototype probes for depth, phantom parameters, and imaging system parameters. Signal to noise ratio will be determined as a function of axial depth into tissue.

Subtask 5.2 Microvascular flow phantom testing (Months 25-30)
Images will be acquired in DFUB mode of microvascular flow phantoms with various diameters. Sinusoidal microvascular phantoms will be imaged at multiple axial depths, as well as with varying flow rates appropriate for simulating tumor microenvironment. A blinded reader study will be performed in which readers rank the sensitivity to slow flow within an added tissue clutter background.

Methods and Results for Task 5: Although much of the in-vitro testing was proposed in year three, we have started these studies in year 2 to provide additional feedback to the design process.

18

In-vitro contrast testing of dual-frequency PC-MUT transducers in water

The harmonic signals from microbubbles (ultrasound contrast agents) were measured using the set-up shown in Figure 18. The micro tube was positioned at about 8 mm away from the transducer. The transmission condition was same as pressure mapping condition (2 MHz, cycles, 300 mV$_{pp}$, and 55dB gain). The cellulose tube was filled with water, air, and micro bubbles, respectively, and then the received signals in each case were processed to obtain echo spectrum and filtered signal. The cut-off frequencies of the high and low pass filters were 10 MHz and 20 MHz, respectively, because the center frequency of the receiver is about 14 MHz. When the water was injected to the micro-tube, no high order harmonic signal reflected from the tube was measured in both raw signal and filtered signal (Figure 19). The peak at fundamental transmitting frequency (2 MHz) in frequency spectrum comes from the electrical coupling and very weak reflected signal from the tube.

The air was next injected to the micro-tube. The reflected waves from the tube due to the large acoustic impedance difference between water and air were detected by the high frequency receiver (Figure 20). The frequency spectrum showed that the received signal has no harmonic components but only fundamental transmitting frequency.
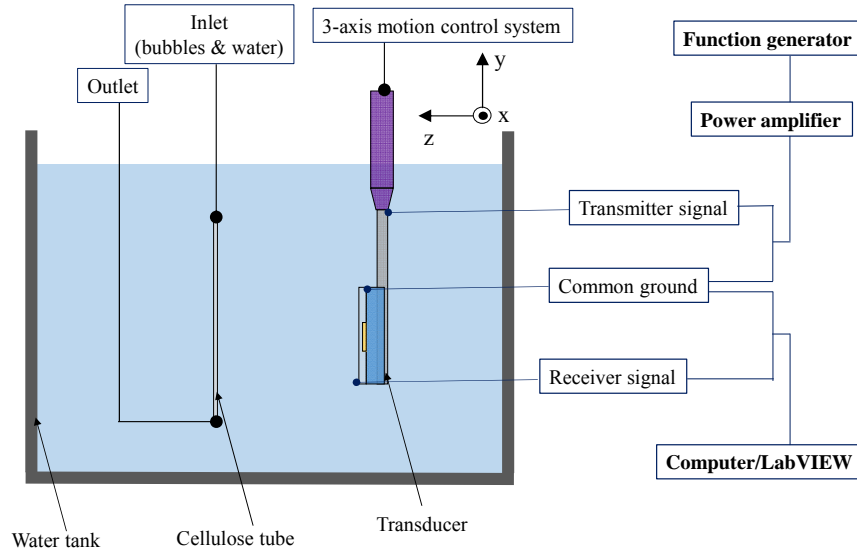

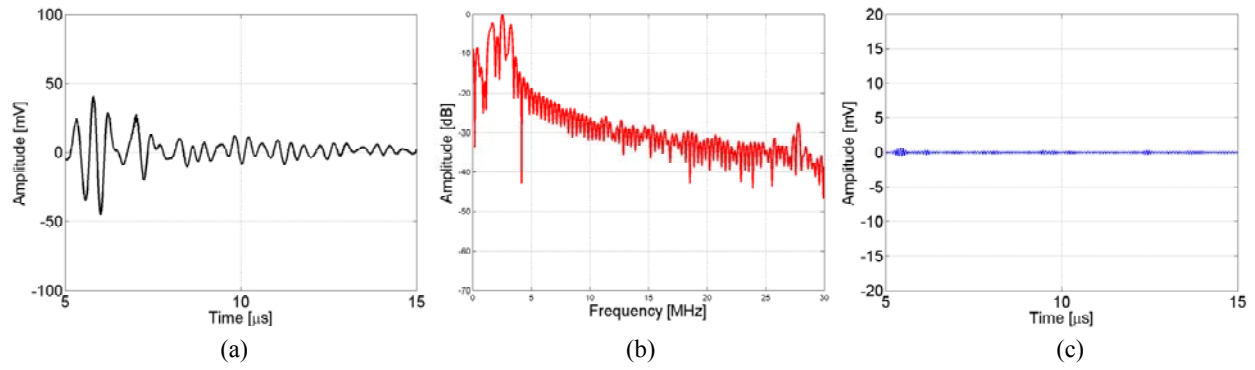**Figure 18.** Bubble signal measurement setup.

Figure 19. Received signal from the tube filled with water: (a) raw signal, (b) frequency spectrum, (c) filtered signal (10 to 20 MHz)
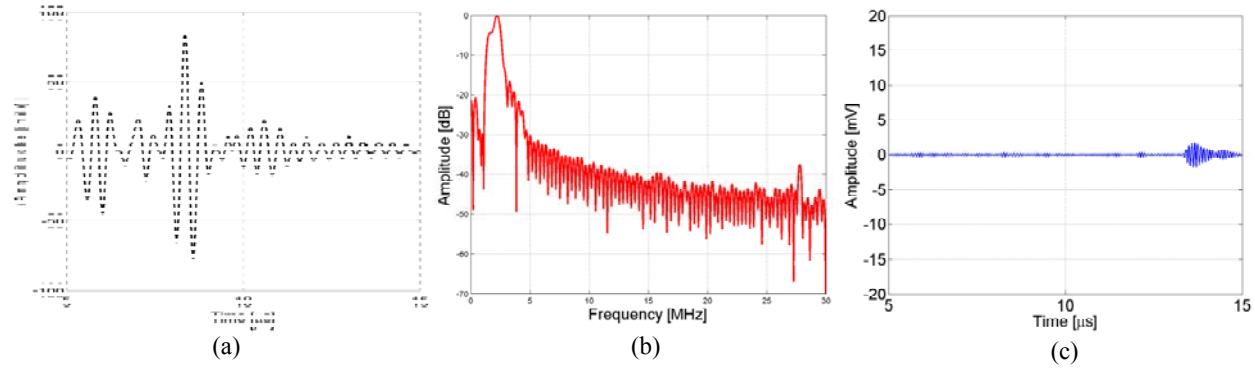

Figure 20. Received signal from the tube filled with air: (a) raw signal, (b) frequency spectrum, (c) filtered signal (10 to 20 MHz).

The diluted microbubbles were then pumped through the tube during the contrast agent detection test. The receiver successfully detected the fundamental reflection and super harmonic responses from the tube filled with microbubbles (Figure 21). The peak amplitude in the raw signal of was slightly reduced, but the frequency spectrum showed distinctive harmonic components. Although the center frequency of the receiver is 14 MHz which means that the receiver has the highest sensitivity for that frequency range and has very low sensitivity at low frequency range as 1 to 4 MHz, the second harmonic component was comparable to the fundamental frequency (-9 dB). The intended receiving frequency components (~14 MHz) also showed in frequency spectrum, and those were slightly larger than 5~10 MHz components. The filtered signal has a discernable peak but the amplitude was not high (5 mV) in comparison with the noise signal. Thus, the bubble response was measured with 16 dB gain and analog high-pass filter which has a cut-off frequency of 10 MHz (Figure 22). With 16 dB gain the harmonic bubble signal showed higher signal-to-noise ratio.
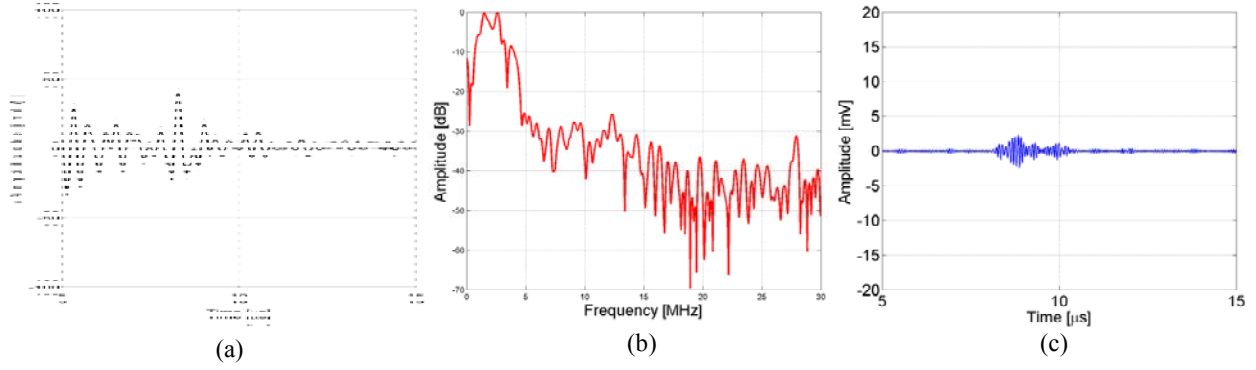
Figure 21. Received signal from the tube filled with bubbles: (a) raw signal, (b) frequency spectrum, (c) filtered signal (10 to 20 MHz).
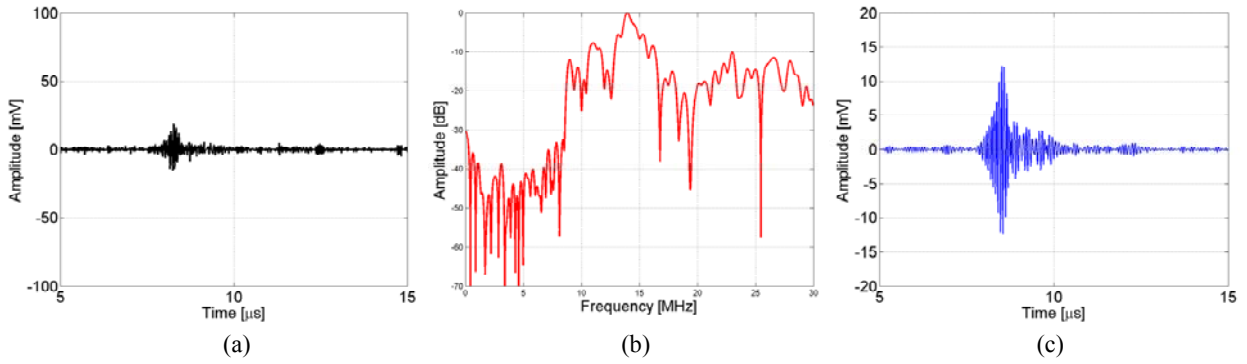

Figure 22. Received bubble signal with 16dB gain and 10 MHz high pass filter: (a) raw signal, (b) frequency spectrum, (c) filtered signal (10 to 20 MHz).

In-vitro phantom testing of dual-frequency PC-MUT transducers

The bubble test was also conducted with a tissue-mimicking phantom. In this experiment, the micro-tube was placed inside of the tissue phantom, which was positioned in the water tank. Other experimental conditions including experiment set-up, settings, and procedure were as the same as the bubble tests using a micro-tube in water.

Phantom fabrication

A graphite-gelatin phantom was used for this study. The phantom composed of 92.5% de-ionized water, 5% n-propanol (to adjust for speed of sound), 2.5% Kodak Photo-Flo 200 (surfactant), 7.5% g/mL porcine gelatin, and 0.115 g/mL graphite. The concentration of graphite was chosen to match experimental attenuation data of normal human prostate of 0.75 dB/cm/MHz. The ingredients were mixed with a stir bar over a stir plate and simultaneously heated to 40-45°C. Once the liquid phantom cooled back down to 30°C, it was poured into the custom mold and refrigerated for 24 hrs. The design of the mold consisted of two parallel cellulose tubes suspended in a hollow rectangular cup, such that if the opening of the cup faced up, the tubes ran parallel to the ground. The cellulose tubes were bound to a larger diameter polyethylene tube

21

using a water-proof adhesive. The distance from the cellulose tube to the surface of the phantom was approximately 5mm, with the tubes being in a distance of 5mm from each other (Figure 23).
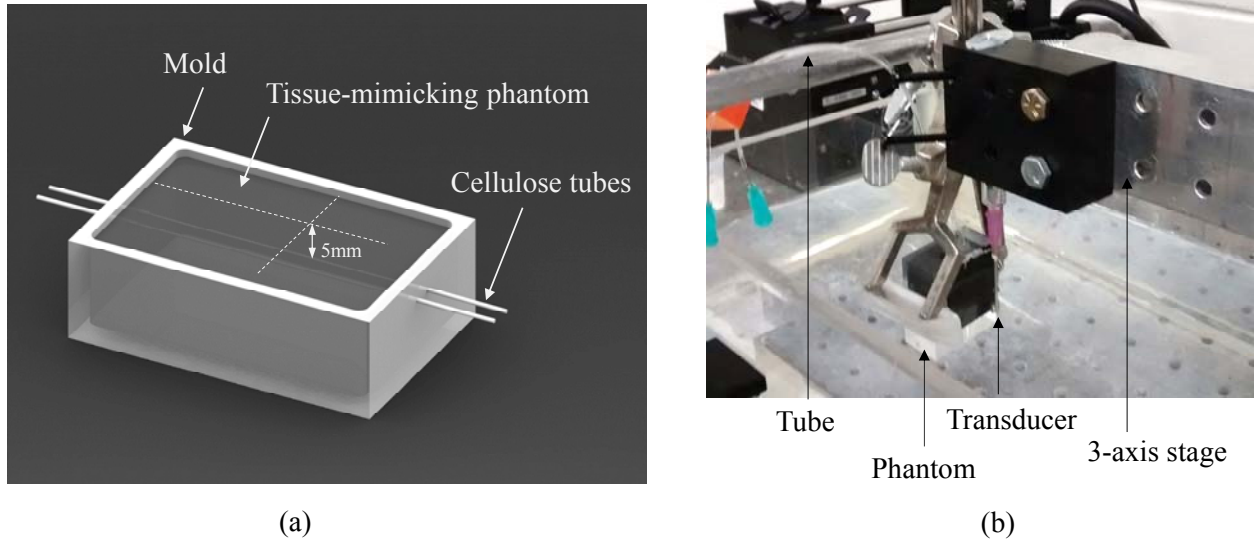

(a)   (b)

Figure 23. Design of a tissue-mimicking phantom

Bubble test results

The reflected signal from the surface of phantom was observed during the bubble test. If the transducer was too close to the phantom, the ringing of reflected signal from the surface was combined with the target signal from the tube. Therefore, to get a clear signal from tube the distance between the tube and the transducer was adjusted to 11 mm (Figure 23 (b)). Firstly, water was injected into microtubes and there was no received signal at the receiver, since the generated waves were almost perfectly transmitted through the tube filled with water (Figure 24). The tube with air showed clear reflected signal without any harmonic components (Figure 25). The micro-bubble case showed clear 7th harmonic signal, as seen in the frequency spectrum (Figure 17). This super harmonic signal was observed even more clearly in filtered signal, but the amplitude was not very high compared to the noise signal from the amplifier (Figure 26 (c)).

We will continue the contrast tests by using an analog high-pass filter (10M Hz) with proper gain (>10 dB).
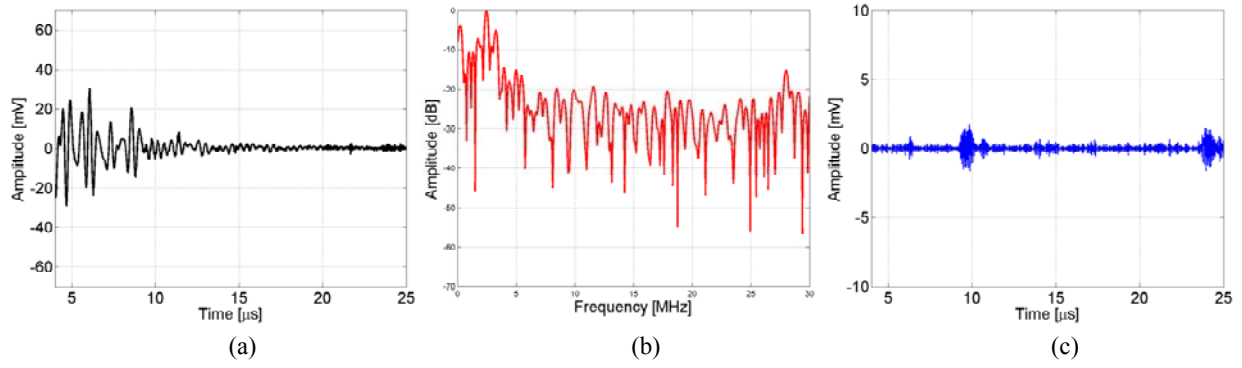
Figure 24. Received signal from the tube filled with water in a phantom: (a) raw signal, (b) frequency spectrum, (c) filtered signal (10 to 20 MHz)
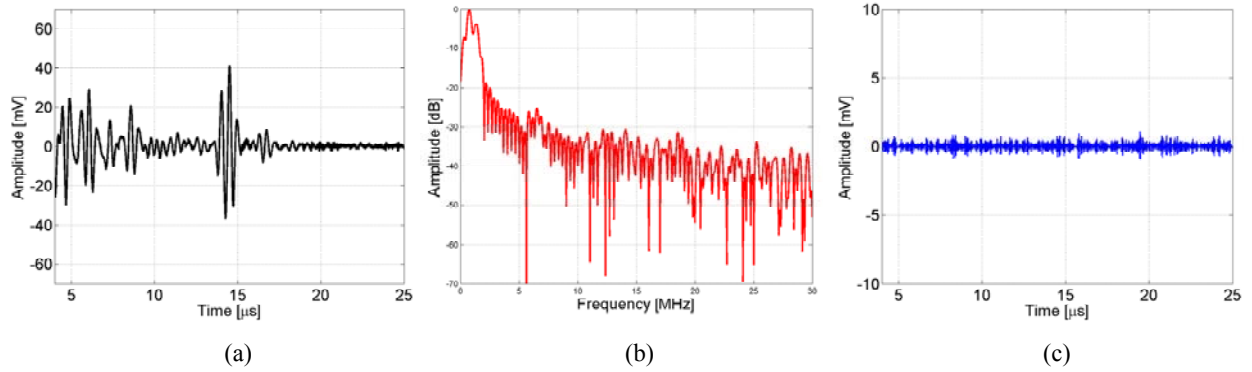

Figure 25. Received signal from the tube filled with air in a phantom: (a) raw signal, (b) frequency spectrum, (c) filtered signal (10 to 20 MHz)
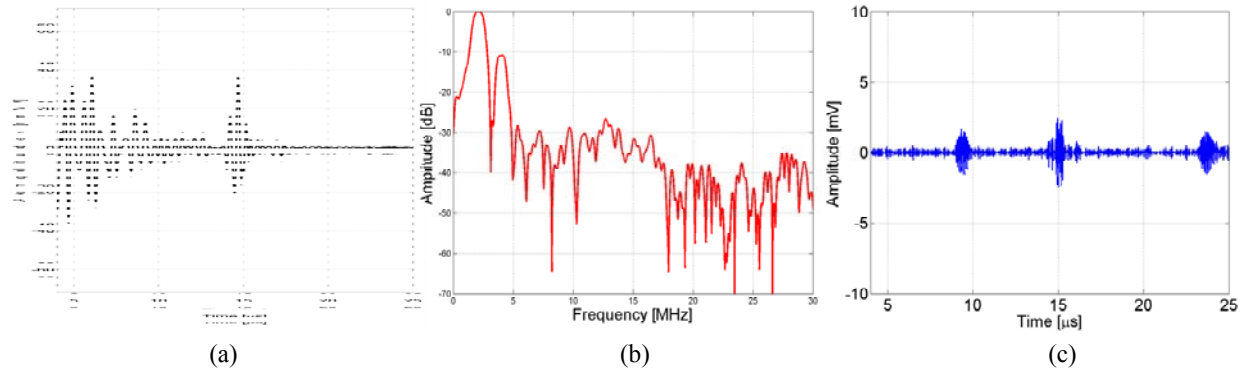

Figure 26. Received signal from the tube filled with bubbles in a phantom: (a) raw signal, (b) frequency spectrum, (c) filtered signal (10 to 20 MHz)

Task 6 In-vivo testing of dual frequency PC-MUT co-linear array (Months 1-6, and 24-36)
Subtask 6.1 Prepare for IACUC approval for animal studies (Months 1-6)

23

Immediately upon project commencement, an appropriate protocol will be prepared for the University of North Carolina *Institutional Animal Care and Use Committee,* for eventual in-vivo imaging studies.

Subtask 6.2 Establish Dunning/Copenhagen rodent prostate cancer model (Months 24-27)
The Dunning R3327 cell line is available from ATCC, from the Johns Hopkins Collection. Twenty 60 day old male Copenhagen Rats (Harlan Indianapolis, IN) will be utilized for in-vivo imaging. Cells will be propagated in culture, and then subcutaneously injected into the flank of each rat. Imaging will be performed starting one week after implantation, and continued until tumors reach approximately 15 mm in diameter, after which animals will be humanely euthanized. For all procedures, animals will be anesthetized using inhaled oxygen and 2% isoflurane. Body temperature will be maintained using a temperature controlled heating pad.

Subtask 6.3 Assess performance of imaging probe in animal model (Months 25-36)
The diagnostic utility of the prototype array to detect cancerous lesions will be assessed in vivo in terms of spatial and temporal sensitivity relative to a conventionally used clinical probe. Two specific imaging approaches will be assessed – ultrasound molecular imaging and microvessel mapping. Spatial sensitivity will be determined by how accurately molecularly targeted contrast agents and microvascular abnormalities conform to the tumor boundaries (relevant to improving biopsy guidance accuracy), while temporal sensitivity will be assessed by observing how these metrics evolve throughout the course of a tumor's growth. The Dunning model will be established in the right flank of 20 male rats (the left flank will serve as a control). To assess the imaging performance of the prototype array as a function of axial depth between 0.5 and 5 cm, tissue mimicking gelatin standoffs will be inserted between the animals' skin and transducer to simulate a deeper lesion depth. Images will be acquired with the clinical probe for contrast imaging of the same tumor and control tissue volumes to compare molecular imaging signal strengths and ability to visualize vascular abnormalities.

Task 6 is to be completed in year 3. No progress yet to report, with the exception of Subtask 6.1, preparation of an IACUC animal protocol. We have prepared this protocol in Year 1.

Task 7 Prepare manuscript for data dissemination (Months 30-36)
Near the end of the project, a second manuscript will be prepared to disseminate imaging results. Likely journal targets will be Ultrasound in Medicine and Biology or IEEE Transactions on Medical Imaging.

Task 7 is to be completed in year 3. No progress yet to report

Key Research Accomplishments

- Single element dual-frequency transducers have been designed, fabricated and tested.
- Contrast imaging tests have been conducted and contrast signals have been successfully detected
- A 24/96-element dual-frequency 2 MHz/20 MHz linear array transducer has been designed and fabricated, and the initial tests have demonstrated promising performance.

Conclusion

Both single element dual frequency transducers and dual frequency linear array transducers designed towards trans-rectal ultrasound imaging have been successfully prototyped and tested.

A single element dual frequency (2 MHz/14 MHz) was designed, fabricated and tested with microbubbles. It was found that: 1) the dual isolation layer works well to block the unwanted background signals; 2) the 1-3 piezoelectric composite is a useful material for the low frequency transmitter without thick and lossy backer, and results in sufficient transmit pressure and reasonably wide bandwidth; and 3) the prototypes based on this design can detect 7th harmonic signal from the micro bubbles.

A dual frequency linear array was developed. The first prototype consists of 24 elements for transmission at 2 MHz and 96 elements for reception at 20 MHz. Electrical impedance and primary acoustic tests have been performed. The low frequency transmission elements were excited by 200 V pulse, and showed a peak-to-peak voltage of 70 mV and -6 dB bandwidth of ~45%. The receiving elements were excited by 1 μJ pulse and showed ~ 300 mV$_{pp}$ response and ~50% in -6 dB bandwidth, respectively.

Prototype dual-frequency transducers demonstrate encouraging performance for contrast enhanced imaging of the prostate.

Publications, Abstracts, and Presentations

Abstract/Presentations

Jinwook Kim, Sibo Li, Xiaoning Jiang "Development of Transmitters in Dual Frequency Transducers for Interventional Contrast Enhanced Imaging", abstract accepted to 2014 IEEE Ultrasonics Symposium, to be presented at the meeting Sept 3-6, 2014.

Publications

K. H. Martin, B Lindsey, J Ma, M. Lee, F. S. Foster, X Jiang, P. A. Dayton, "Dual-frequency Transducers for Contrast Enhanced Ultrasound Imaging", *Sensors*, In Review

Inventions, Patents, and Licenses

Nothing to report

Reportable Outcomes

Nothing to report

Other Achievements

Nothing to report

References

1. Ma, J., K. Martin, P. Dayton, X. Jiang, "A preliminary engineering design of intravascular dual-frequency transducers for contrast enhanced acoustic angiography and molecular imaging", *Ultrasonics, Ferroelectrics and Frequency Control, IEEE Transactions on* , 61(5), 870-80 (2014).

Appendices

Nothing to report